

Closed-form solutions for the Lévy-stable distribution

Karina Arias-Calluari^[1],* Fernando Alonso-Marroquin^[1,2], and Michael S. Harré^[3]

[1]School of Civil Engineering, The University of Sydney, Sydney NSW 2006

[2]Computational Physics IfB, ETH Zurich, CH-8093, Zurich, Switzerland and

[3]Complex Systems Research Group, The University of Sydney, Sydney NSW 2006

(Dated: July 3, 2018)

The Lévy-stable distribution is the attractor of distributions which hold power laws with infinite variance. This distribution has been used in a variety of research areas, for example in economics it is used to model financial market fluctuations and in statistical mechanics as a numerical solution of fractional kinetic equations of anomalous transport. This function does not have an explicit expression and no uniform solution has been proposed yet. This paper presents a uniform analytical approximation for the Lévy-stable distribution based on matching power series expansions. For this solution, the trans-stable function is defined as an auxiliary function which removes the numerical issues of the calculations of the Lévy-stable. Then, the uniform solution is proposed as a result of an asymptotic matching between two types of approximations called “the inner solution” and “the outer solution”. Finally, the results of analytical approximation are compared to the numerical results of the Lévy-stable distribution function, making this uniform solution valid to be applied as an analytical approximation.

I. INTRODUCTION

A wide range of natural and social phenomena exhibit a power-law in the probability distribution of large events. These tails are characterized by the asymptotic relation $f(x) \sim 1/x^{1+\alpha}$, where x is the size of the events [1, 2]. For $0 < \alpha \leq 1$, the distribution has an indefinite mean value. On the other hand, for $1 < \alpha \leq 2$, the distribution has a defined mean value but still exhibits infinite variance [3]. These heavy-tailed distributions have been observed in economics and statistical mechanics.

In the field of economics, the statistics of price returns, trade size, and share volumes have been investigated. Heavy tailed distributions have been observed in the correlations of the absolute value of the S&P 500 returns [4, 5], the effects of networks on price returns [6], daily returns of the Dow Jones index [7], Brent crude oil returns [8] and the aggregate output growth rate distribution [9]. Even after applying five different estimation techniques, power law tails with the characteristic index α were found on the cumulative distribution of trade size and share volumes of 252 US stocks over the 42-year period from 1963-2005 [10, 11]. To capture heavy tails different models have been proposed to simulate the stock price dynamics. For instance, models of anomalous diffusion of option pricing were introduced as an extension of the well-known Brownian model [12, 13]. These models are focused on different aspects such as capturing the dynamic of the price with waiting times (periods of stagnation) which are Lévy-stable distributed [12] or on the effect of “particles” representing agent’s interaction [13]. The continuous counterpart of these discrete models is the Fokker-Planck equation (FPE) that is presented in terms of fractional derivatives. The solution of FPE gives the time evolution of the probability density function (pdf) of price return [12–14].

In the field of statistical mechanics, the diffusion equation (DE) is a fundamental equation of transport dynam-

ics used to describe a particle motion resulting from the interaction with a thermal heat bath [15–17]. The DE defines the probability of a particle to be at a certain position at a specific time, and its pdf is given by the Gaussian distribution [18–20]. On the other hand, for the generalization of anomalous transport, a fractional diffusion equation (FDE) is used to describe a continuous time random walk (CTRW) model [16, 21]. This model generalizes the Brownian diffusion motion based on two parameters accounting for the jump length and the waiting time between two successive jumps. A long-tailed waiting time pdf—long rests—, produces a “subdiffusion process” [16, 17]. On the opposite case, the Lévy-stable distribution for the jump length pdf—long jumps— produces a “superdiffusion process” [16, 22]. The anomalous diffusion under an external velocity field or a microscopic advection is studied by fractional diffusion-advection equations (FDAE) [16, 17, 23]. Additionally, the fractional Fokker-Planck equation (FFPE) is used to study the anomalous diffusion under the influence of an external field: electrical bias field [16, 17], periodic potentials [24, 25] or a harmonic potential [18, 21, 26]. The FFPE can be derived either from the generalized FDE of continuous time random walk models or from a Langevin equation with Lévy-stable noise or gaussian noise and long rests [18, 25, 27].

The previous fractional kinetic equations (FDE, FDAE and FFPE) can be solved in terms of Lévy-stable distribution function that has an analytical solution for only two cases—the normal and Cauchy distributions—[28]. In the remaining cases there is not a closed-form expression. Typically the numerical solution of the Lévy-stable distribution has numerical oscillations in the tail of the distribution. For some cases it displays apparent discontinuity in logarithmic plots because of negative values obtained from the numerical solution [29]. Consequently numerical solutions of the Lévy-stable distribution are not reliable as the probability density function must be positive.

Analytical expressions in terms of power series have been presented by different authors. Feller [30], Elliot

* School of Civil Engineering; kari0293@uni.sydney.edu.au

[31] and Zolotarev [32] used power series to obtain converging algorithms of the Lévy-stable distribution function in two ranges, the first for $\alpha < 1$ and the second for $\alpha > 1$ for symmetric distributions. However, some of the proposed series do not converge to the Lévy-stable function, and some of them are only applicable for extreme values $x \rightarrow 0$ or $x \rightarrow \infty$. Mantegna [33] presented a similar solution that of Elliot [31] but the algorithm is only valid when $x \rightarrow \infty$ and $0.75 < \alpha \leq 1.95$. Nolan [34] presented an algorithm for asymmetric distributions of large events $x \rightarrow \infty$ focusing only on the tail behaviour of the distribution. Thus, the Lévy-stable distribution function does not have an explicit expression [35, 36] and no uniform solution of the Lévy-stable distribution has been proposed until now [30, 32, 34].

Due to the absence of an explicit expression, numerical solutions were developed to evaluate the Lévy-stable distribution function by using numerical recursive quadrature methods [37–39]. Nolan [37, 40] develops a numerical solution for the estimation of Lévy-stable parameters through a maximum likelihood method for each data set of x . However, Nolan’s method converges only for $\alpha > 0.4$ and the convergence to the Lévy-stable distribution function seems to be not accurate enough. Despite this fact, Nolan’s method constitutes an important method that is still being used [38].

Apart from the numerical issues in the evaluation of the Lévy-stable distribution, some authors have pointed out its infinite variance as a drawback [41–43]. To avoid the infinite variance of the Lévy-stable distribution function, several truncations are proposed. The truncation was justified by the observed change of slope of the tails on extensive datasets [44]. For example, when evaluating the returns per minute of S&P 500 index data over the ten year period from 1985–95 a change of slope from $\alpha = 1.4$ to $\alpha = 3$ was found. The truncations make the variance finite, consequently the distribution function of the sum of independent random variables converges to the normal distribution due to the central limit theorem for large N . Nevertheless, a time series in some stock market indices can exhibit infinite variance, one such case is the variance of price fluctuations in Shanghai stock market index, which increases when the time frame is enlarged [45, 46].

The aim of this paper is to formulate a uniform analytical approximation for the Lévy-stable distribution function based on a series expansion. To achieve this aim we propose several regularizations of the inner and outer series expansions to ensure convergence. This will be an important tool to get the most accurate approximation reducing numerical errors (oscillations) when the Lévy-stable function is evaluated.

This paper is divided in two parts. The first part introduces the Lévy-stable distribution and the trans-stable function. They are defined by Fourier transformations in sections III and IV respectively. The trans-stable function is shown to be identical to the Lévy-stable distribution for $\alpha < 1$ and it has the same asymptotic behaviour

for $\alpha > 1$ for large events. The second part refers to section V and it deals with the closed form— analytical approximations— of the Lévy-stable distribution. For this purpose, two types of approximations are developed. The first approximation refers to the inner expansion that converges asymptotically to the Lévy-stable distribution as $x \rightarrow 0$. The second approximation refers to the outer expansion that converges asymptotically as $x \rightarrow \infty$. For the outer expansion two cases are presented, one is obtained from the Lévy-stable function in subsection VB and the second one from the trans-stable function in subsection VC. Finally, the uniform solution in section VI is proposed as a result of matching the inner and the outer solution. The analytical equation of uniform solution proposed in this paper gives an approximated solution of the Lévy-stable distribution function over the range $-\infty < x < \infty$.

II. CENTRAL LIMIT THEOREM FOR LÉVY-STABLE FLIGHTS

Section 35 of the book by Gnedenko and Kolmogorov [47] shows that the normal distribution is an “attractor” of distributions with finite variances. On the other hand, the attractor of power law distributions with infinite variances corresponds to the more general “Lévy-stable law”. In other words the Lévy-stable is a specific function to which other distributions converge.

The fundamental concept of attractors is formulated as follows. If a normalized sum of a set of independent, identically distributed random variables $\{X_1, X_2, X_3 \dots X_N\}$ satisfies:

$$\lim_{N \rightarrow \infty} \frac{1}{\sigma_N} \left(\sum_{i=1}^N X_i - \mu_N \right) = X, \quad (1)$$

then X belongs to the stable law. The coefficients μ_N and σ_N represent the centering and normalizing values respectively [47].

The Gnedenko-Kolmogorov theorem is a generalization of the classical central limit theorem which states that normalized sum of independent random variables with finite variance in Eq. (1) converges to a variable that is normally distributed [47, 48]. This is the case of distributions with power-law tails ($\alpha \geq 2$) with finite variance. The normalized coefficient is $\sigma_N = \sqrt{N}$ and the centering coefficient is $\mu_N = NE[X]$, where N represents the length of the sum and $E[X]$ refers to expected value [49, 50]. On the other hand, for independent random variables power law distributions with infinite variances ¹ $0 < \alpha < 2$, Uchaikin and Zolotarev [32, 50] show that

¹Note: Infinite variance is observed for $0 < \alpha < 2$. This characteristic occurs for $0 < \alpha \leq 1$, as a consequence of not having a well-defined expected value $E[X]$. For $1 < \alpha < 2$, the integral in the variance definition diverges [30, 32, 50].

X in Eq. (1) follows a symmetric Lévy-stable law if the normalization coefficient is $\sigma_N = N^{1/\alpha}$ and the centering coefficient is $\mu_N = 0$ for $\alpha \leq 1$ or $\mu_N = NE[X]$ for $\alpha > 1$.

Lévy-stable distributions belong to a wider class of infinitely divisible distributions (ID). A random variable X is ID if it can be represented as the sum of a number N of independent and identically distributed random variables with a common law (N) [51], i.e.:

$$X = \sum_{i=1}^N Y_i^{(N)} \quad \forall \quad N \in \mathbb{N} \quad (2)$$

The pdf of X is $f(x)$. If $f(x)$ is Lévy-stable, then $f(x)$ is an ID distribution function. The proof of this statement is obtained by replacing $Y_i^{(N)} = (X_i - \mu_N)/\sigma_N$ into Eq. (2). Then, by applying the limit $N \rightarrow \infty$ Eq. (1) is obtained. An equivalent definition of ID can be given in terms of the characteristic function. The characteristic function is defined as the Fourier transform of the probability density function $f(x)$,

$$\varphi(t) = \mathbb{E}(e^{itx}) = \int_{-\infty}^{\infty} f(x)e^{itx} dx. \quad (3)$$

The characteristic function of the ID distribution can be derived as follows. Consider X as a sum of two independent random variables $X = Y_1 + Y_2$ with pdf's $f_1(x)$ and $f_2(x)$ respectively. For the convolution of the two probability distributions [43], the pdf of X has the form,

$$f(x) = \int_{-\infty}^{\infty} f_1(k)f_2(x-k)dk. \quad (4)$$

By substituting Eq. (4) into Eq. (3) and interchanging the order of the integration the equation for the characteristic function of X is obtained,

$$\varphi_X(t) = \varphi_{Y_1}(t)\varphi_{Y_2}(t). \quad (5)$$

Assuming that Y_1 and Y_2 are identically distributed, the characteristic function of $f(x)$ can be defined as $\varphi_X(t, 2) = (\varphi(t))^2$. In general, for the sum of N independent and identically distributed random variables in Eq. (2), the characteristic function is given by:

$$\varphi_X(t, N) = (\varphi_N(t))^N. \quad (6)$$

Consequently, Eq. (2) and Eq. (6) are equivalent. Then, the limit is applied in Eq. (6), $\varphi_X(t) = \lim_{N \rightarrow \infty} \varphi_X(t, N)$. As a consequence, $\varphi_X(t)$ is the characteristic function of the pdf of the random variable X . This statement constitutes the Levy continuity theorem that guarantees pointwise convergence [51, 52]. The Lévy-Khintchine formula or Triple Lévy gives the general equation for ID distributions [51]. This formula determines the class of characteristic function where the pdf is calculated from its Fourier transform [52–55]. The Lévy-stable distribution constitutes a special case of the general Lévy-Khintchine in one-dimensional case that is presented in the next section [52].

III. LÉVY-STABLE DISTRIBUTION FUNCTION

The Lévy-stable distribution is given by the Fourier transform of Eq. (3),

$$f(x; \alpha, \beta, \sigma, \mu) = \frac{1}{2\pi} \int_{-\infty}^{\infty} \varphi(t; \alpha, \beta, \sigma, \mu) e^{ixt} dt. \quad (7)$$

Where $\varphi(t)$ is presented in Section 34 of the Gnedenko-Kolmogorov book [47] as,

$$\varphi(t; \alpha, \beta, \sigma, \mu) = e^{(it\mu - |\sigma t|^\alpha (1 - i\beta \operatorname{sgn}(t)\Phi))}. \quad (8)$$

The four parameters involved are: the stability parameter $\alpha \in (0, 2]$, the skewness parameter $\beta \in [-1, +1]$, the scale parameter $\sigma \in (0, +\infty)$, and the location parameter $\mu \in (-\infty, +\infty)$. The parameter α constitutes the characteristic exponent of the asymptotic power-law in the tails and it determines whether the mean value and the variance exist. The Lévy-stable distribution with $0 < \alpha \leq 1$ does not have a mean value and it has a define variance only for $\alpha = 2$ [56].

The function $\operatorname{sgn}(t)$ represents the sign of t and the function Φ is defined as:

$$\Phi = \begin{cases} \tan\left(\frac{\pi\alpha}{2}\right) & \alpha \neq 1, \\ -\frac{2}{\pi} \log|t| & \alpha = 1. \end{cases} \quad (9)$$

The Lévy-stable distribution is the family of all attractors of normalized sums of independent and identically distributed random variables. The most well-known Lévy-stable distribution functions are the Cauchy distribution with $\alpha = 1$ and the normal distribution function with $\alpha = 2$. Both functions have $\beta = 0$, which means they are symmetric distributions about their mean [32].

In this paper we will focus on symmetric distributions. For this case the Lévy-stable distribution can be normalized as follows:

$$f(x; \alpha, \beta = 0, \sigma, \mu) = \operatorname{Re} \left\{ S \left(\frac{x - \mu}{\sigma}, \alpha \right) \right\}, \quad (10)$$

where the general distribution function is given by the following equation:

$$S(x; \alpha) = \frac{1}{\pi} \int_0^{\infty} e^{-t^\alpha} e^{ixt} dt. \quad (11)$$

The real part of this function corresponds to the normalized Lévy-stable distribution,

$$s(x; \alpha) = \operatorname{Re}(S(x; \alpha)).$$

Consequently, by applying Euler's formula we arrive at [57]:

$$s(x; \alpha) = \frac{1}{\pi} \int_0^{\infty} e^{-t^\alpha} \cos(tx) dt. \quad (12)$$

IV. TRANS-STABLE FUNCTION

Zolotarev (1986) used the term “trans-stable” to refer to a power series expansion that converges to the Lévy-stable distribution for $0 < \alpha < 1$ only [32]. In this paper, trans-stable is the function which one of its solutions originates Zolotarev series when the series expansions are applied around $x \rightarrow \infty$. First we define the *complex trans-stable function* in the range of $0 < \alpha < 2$. For $\alpha < 1$, the Lévy-stable distribution and the trans-stable function are identical. For $\alpha > 1$, the trans-stable function and the Lévy-stable distribution present the same asymptotic behaviour for $x \rightarrow \infty$. Consequently, our trans-stable function can be used to find a numerical approximation of the Lévy-stable distribution function for $\alpha > 1$ for large events.

First, the *complex trans-stable function* is defined as an integral over the path C in the complex plane:

$$G_C(x; \alpha) = \frac{1}{\pi} \int_C I(x, z; \alpha) dz, \quad (13)$$

where

$$I(x, z; \alpha) = e^{-z^\alpha} e^{ixz}. \quad (14)$$

The relation of this function to the Lévy-stable $S(x; \alpha)$ and the trans-stable $T(x; \alpha)$ functions is obtained by choosing a particular path C in the complex plane. Then, the Lévy-stable distribution and trans-stable function are given by Eq. (15) and (16) respectively:

$$S(x; \alpha) = G_{[0, \infty)}(x; \alpha) = \frac{1}{\pi} \int_0^\infty e^{-t^\alpha} e^{ixt} dt, \quad (15)$$

$$T(x; \alpha) = G_{[0, i\infty)}(x; \alpha) = \frac{1}{\pi} \int_0^{i\infty} e^{-t^\alpha} e^{ixt} dt. \quad (16)$$

First it will be shown that for $0 < \alpha \leq 1$, both Lévy-stable $S(x; \alpha)$ and trans-stable $T(x; \alpha)$ functions are identical. For $1 < \alpha < 2$ it will be demonstrated that both functions exhibit the same asymptotic behaviour when $x \rightarrow \infty$.

This demonstration is based on the evaluation of the *complex trans-stable integral* Eq. (13) using polar representation for $\alpha \leq 1$ and rectangular representation for $\alpha > 1$ on the complex integrand. The demonstrations are presented in the following subsections.

1. For $0 < \alpha \leq 1$

Here we will show that for $0 < \alpha \leq 1$ the Lévy-stable and trans-stable functions are identical. This demonstration will be done by considering the closed contour shown

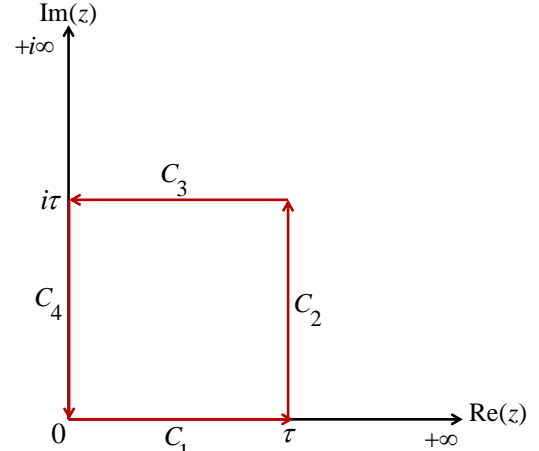


Figure 1. Contour integration for Eq. (13)

in Figure 1. Since the complex function in Eq. (14) is analytical over the complex plane, the integral over the closed contour Eq. (13) is zero,

$$\oint I(x, z; \alpha) dz = 0. \quad (17)$$

Let us take the contour in Figure 1 that can be divided into four straight paths so that:

$$\sum_{i=1}^4 \int_{C_i} I(x, z; \alpha) dz = 0. \quad (18)$$

Now, we will take the limit when $\tau \rightarrow \infty$ in Figure 1. Using Eq. (15,16,18) the following equation is obtained:

$$S(x; \alpha) - T(x; \alpha) = -\lim_{\tau \rightarrow \infty} \sum_{i=2}^3 \int_{C_i} I(x, z; \alpha) dz. \quad (19)$$

To evaluate the right hand side in Eq. (19) it is convenient to use the polar representation of the complex number $z = re^{i\theta}$ and express Eq. (14) in polar coordinates:

$$I(x, z; \alpha) = e^{g(x, r, \theta; \alpha) + ih(x, r, \theta; \alpha)}, \quad (20)$$

$$g(x, r, \theta; \alpha) = -r^\alpha \cos(\theta\alpha) - rx \sin \theta, \quad (21)$$

$$h(x, r, \theta; \alpha) = -r^\alpha \sin(\theta\alpha) + rx \cos \theta. \quad (22)$$

It will be adopted the nomenclature of signal theory, where the polar notation separates the effects of instantaneous amplitude $|I| = e^g$ and its instantaneous phase h of a complex function [58]. Consequently, $g(x, r, \theta; \alpha)$ represents the *attenuation factor* and $h(x, r, \theta; \alpha)$ represents the *oscillation factor*.

Now let us notice that $\lim_{r \rightarrow \infty} g(x, r, \theta; \alpha) = -\infty$ for $0 < \alpha \leq 1$ at any value of x . This statement is based on the fact that $\cos(\theta\alpha) \geq 0$ in the first quadrant for $\alpha \leq 1$. Consequently, $\lim_{r \rightarrow \infty} I(x, z; \alpha) = 0$ so that the integral of the right side of the Eq. (19) vanishes at $\tau \rightarrow \infty$, therefore:

$$S(x; \alpha) = T(x; \alpha) \quad \text{if } 0 < \alpha \leq 1. \quad (23)$$

So, the Eq. (23) will allow to use the trans-stable function $T(x; \alpha)$ instead of the Lévy-stable distribution function $S(x; \alpha)$ for $0 < \alpha \leq 1$ in the numerical integration. This is with the aim to remove numerical oscillation, specifically in the tails. It is noticeable that the integration of the trans-stable function $T(x; \alpha)$ in Eq. (16) is performed over the imaginary axis. Applying the following change of variable $t \rightarrow -it$ (formally done by defining $u = -it$ so that $du = -idt$ and later replacing the dummy variable u by t inside the integral), the trans-stable function is converted into a Laplace transformation. Consequently, the integration is performed over the real axis. The Fourier and Laplace representations for $T(x; \alpha)$ are shown in Eq. (24),

$$T(x; \alpha) = \frac{1}{\pi} \int_0^{i\infty} e^{-t^\alpha} e^{ixt} dt = \frac{1}{\pi} \int_0^\infty e^{-(it)^\alpha} e^{-xt} idt. \quad (24)$$

Figure 2 compares the Fourier representation of the Lévy-stable distribution function $S(x; \alpha)$ and the Laplace representation of trans-stable function $T(x; \alpha)$. The integration is performed using a recursive adaptive Simpson quadrature method [59]. It is evident that the Laplace representation removes the oscillations of the Fourier representation of the Lévy-stable distribution for $\alpha < 1$.

It is important to add that the Lévy-stable distribution function and trans-stable function hold the same value for their Fourier and Laplace transform representations. The difference between each transform representation is the axis in which each function is integrated. The expressions are shown in Table I.

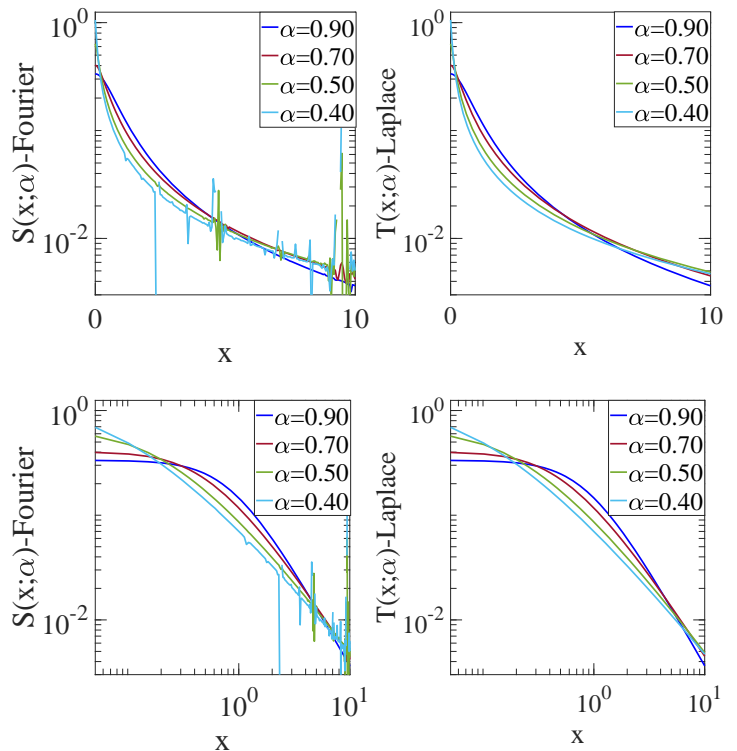


Figure 2. Comparison of numerical integration $0 < \alpha < 1$ between Fourier and Laplace transform of the Lévy-stable $S(x; \alpha)$ and the trans-stable $T(x; \alpha)$ functions using recursive adaptive Simpson quadrature method [59]. The absolute error tolerance of the method is $\xi = 3.5 \times 10^{-8}$. Top plots are shown in semi-logarithmic scale and in logarithmic scale.

	Lévy-stable distribution $S(x; \alpha)$	Trans-stable function $T(x; \alpha)$
Fourier transform	$\frac{1}{\pi} \int_0^\infty e^{-t^\alpha} e^{ixt} dt$	$\frac{1}{\pi} \int_0^{i\infty} e^{-t^\alpha} e^{ixt} dt$
Laplace transform	$\frac{1}{\pi} \int_0^{-i\infty} e^{-(it)^\alpha} e^{-xt} idt$	$\frac{1}{\pi} \int_0^\infty e^{-(it)^\alpha} e^{-xt} idt$

Table I. Summary of Fourier and Laplace representations for the Lévy-stable and the trans-stable functions

2. For $1 < \alpha < 2$

Here we will show that for $1 < \alpha < 2$ the Lévy-stable and trans-stable functions have the same asymptotic behaviour on large events if the integrals are appropriately truncated.

Let us recall Eq. (21) for the *attenuation factor*,

$$g(x, r, \theta; \alpha) = -r^\alpha \cos(\theta\alpha) - rx \sin \theta.$$

In the previous section, it was shown that $\cos(\theta\alpha)$ is always positive in the first quadrant of the complex plane if $0 < \alpha \leq 1$. Otherwise, if $\alpha > 1$, then $\cos(\theta\alpha) < 0$ when $\theta = \pi/2$. Consequently, $\lim_{r \rightarrow \infty} I(x, r, \theta; \alpha) = \infty$ in this

range, so that the right hand side of Eq. (19) can not be neglected. Therefore $S(x) \neq T(x)$ if $\alpha > 1$.

We can find an approximation between these two functions if the τ value in the contour of Figure 1 is kept large but finite ($\tau < \infty$). Thus, Eq. (18) becomes:

$$S(x; \alpha, \tau) - T(x; \alpha, \tau) = - \sum_{i=2}^3 \int_{Si} I(x, z; \alpha) dz, \quad (25)$$

where $S(x; \alpha, \tau)$ and $T(x; \alpha, \tau)$ are the truncated integrals in Eqs. (15) and (16) respectively:

$$S(x; \alpha, \tau) = \frac{1}{\pi} \int_0^{\tau} e^{-t\alpha} e^{ixt} dt, \quad (26)$$

$$T(x; \alpha, \tau) = \frac{1}{\pi} \int_0^{i\tau} e^{-t\alpha} e^{ixt} dt. \quad (27)$$

Now, the right hand of Eq. (25) can be evaluated in the limit where $x \rightarrow \infty$. First, notice that in the contour of integration in Figure 1 the magnitude of r is bounded by the condition $0 < r < \sqrt{2} \tau$ and $\sin(\theta) > 0$ in the first quadrant, thus:

$$\lim_{x \rightarrow \infty} g(x, r, \theta; \alpha) = -\infty.$$

Consequently, $\lim_{x \rightarrow \infty} I(x, z; \alpha) = 0$ so that the integral on the right of Eq. (25) vanishes at $x \rightarrow \infty$. Therefore, the asymptotic behaviour is obtained for $1 < \alpha < 2$,

$$S(x; \alpha, \tau) \sim T(x; \alpha, \tau) \quad \text{as } x \rightarrow \infty. \quad (28)$$

This demonstrates that both functions are asymptotically equivalent when the integrals are truncated.

The next step is to find the truncation value τ that leads to the best approximation of these functions. The value of τ should be chosen to minimize the truncation error and at the same time to make the domain of integration as small as possible. With this aim, the trans-stable function $T(x; \alpha, \tau)$ in Eq. (16) is expressed in its Laplace representation by using the change of variable $t \rightarrow -it$. Thus,

$$T(x; \alpha, \tau) = \frac{1}{\pi} \int_0^{\tau} \bar{I}(x, t; \alpha) dt, \quad (29)$$

where \bar{I} corresponds to Laplace transform integrand shown in Eq. (24) and Table I,

$$\bar{I}(x, t; \alpha) = e^{(-it)\alpha} e^{-xt}. \quad (30)$$

Then, considering Euler's representation for a complex exponential function $e^{i\theta} = \cos(\theta) + i\sin(\theta)$, the following equations are obtained to express Eq. (30):

$$\bar{I}(x, t; \alpha) = e^{\bar{g}(x, t; \alpha) + i\bar{h}(x, t; \alpha)}, \quad (31)$$

$$\bar{g}(x, t; \alpha) = -t\alpha \cos\left(\frac{\pi\alpha}{2}\right) - xt, \quad (32)$$

$$\bar{h}(x, t; \alpha) = -t\alpha \sin\left(\frac{\pi\alpha}{2}\right) + \frac{\pi}{2}. \quad (33)$$

The instantaneous amplitude $|\bar{I}| = e^{\bar{g}}$ will be determined by the *attenuation factor* in Eq. (32). For that reason, an analysis of $\bar{g}(x, t; \alpha)$ was made in Figure 3. The curve $\bar{g}(x, t; \alpha) = 0$ divides two regions, one with exponential growth ($\bar{g} > 0$) and the other with exponential decay ($\bar{g} < 0$).

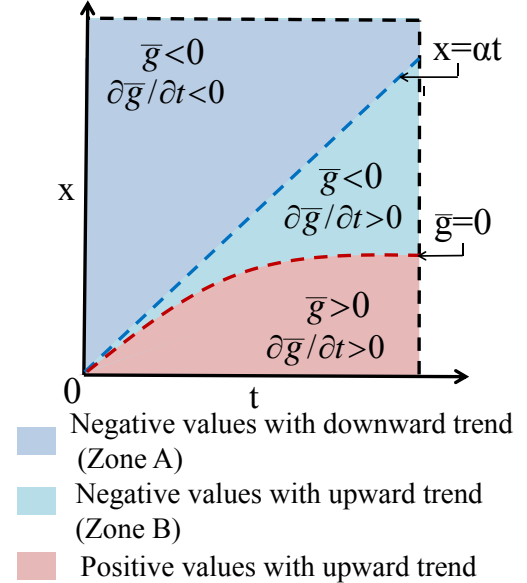


Figure 3. Curve $\bar{g} = 0$ separates two regions with $\bar{g} > 0$ and $\bar{g} < 0$. In the latter region, two zones can be distinguished: zone A with $\partial\bar{g}/\partial t < 0$ and zone B with $\partial\bar{g}/\partial t > 0$. The equation $x = \alpha t$ is an estimation of the boundary between zones A and B.

In Figure 3, two sub-regions can be recognized in $\bar{g} < 0$. The first one, “Zone A” which contains negative \bar{g} values with downward trend $\partial\bar{g}/\partial t < 0$ that is faster as $x \rightarrow \infty$. The second sub-region is “Zone B”, it contains smaller negative \bar{g} values that follow an upward trend and $\partial\bar{g}/\partial t > 0$ displaying an increase behaviour when $x \rightarrow 0$. Considering these sub-regions, the truncation τ in Eq. (29) will depend on x value as follows:

- For $x \rightarrow 0$, The integration must avoid zone B. The values of $\bar{g}(x, t; \alpha)$ in this zone lead to an exponential growth due to an upward trend $\partial\bar{g}/\partial t > 0$, consequently $|\bar{I}| \rightarrow 0$.
- For $x \rightarrow \infty$, the integration should be restricted to zone A. The downward trend $\partial\bar{g}/\partial t < 0$ leads to obtain $\bar{g}(x, t; \alpha) \rightarrow 0$. Consequently, the convergence of $|\bar{I}| \rightarrow 0$ occurs faster as $t \rightarrow \infty$.

For $x \rightarrow 0$, the cut off τ_1 which avoids most of zone B is defined by $x = \alpha t$. This equation is an estimation of

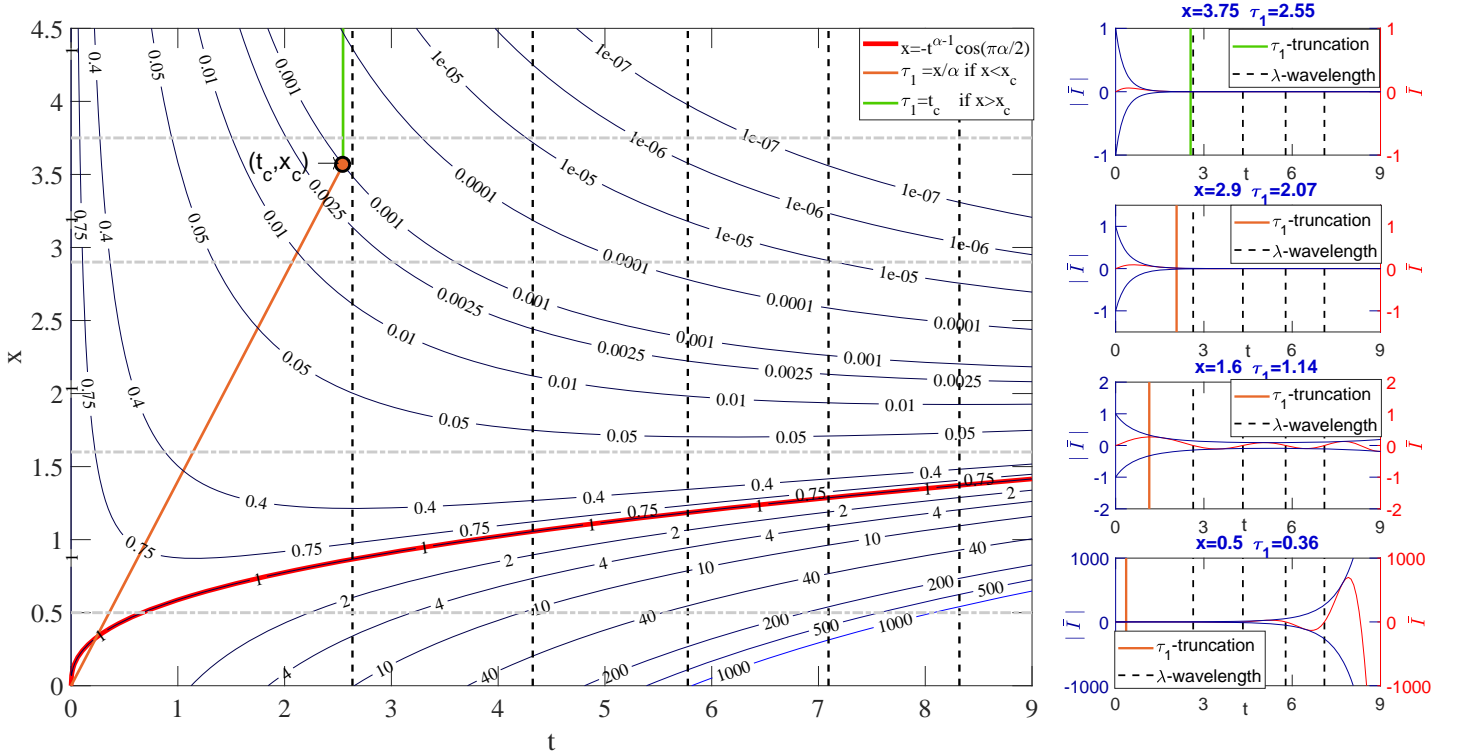


Figure 4. Contour plot of $e^{\bar{g}}$ that represents the instantaneous amplitude $|\bar{I}|$ for $\alpha = 1.4$ and tolerance $\epsilon = 10^{-3}$ in Eq. (31) and (32). The red line x was drawn by considering $\bar{g} = 0$ which represents the limit between the positive and negative values of the attenuation factor \bar{g} . The truncation τ_1 is applied following Eq. (35). Downward trend before τ_1 and upward trend after τ_1 of $|\bar{I}|$ can be observed in the right part of the figure for $x = 0.5$ and $x = 1.6$. For $x = 2.9$ and $x = 3.8$ the truncation is made after reaching a small value on the modulation \bar{I} .

the boundary between zones A and B for all range of α values.

The cut off τ_1 obeys a linear equation and is obtained from the following equations:

$$e^{\bar{g}(x, \tau_1; \alpha)} = |\bar{I}| = \epsilon \text{ and } x = \alpha \tau_1, \quad (34)$$

where the tolerance ϵ represents a negligible instantaneous amplitude $|\bar{I}|$.

For $x \rightarrow \infty$, the cut off τ_1 will restrict the integration of \bar{I} on a closed interval $[0, t_c]$. This occurs due to a faster downward trend $\partial g / \partial t < 0$. The t_c value represents the point where the instantaneous amplitude can be considered a negligible quantity $|\bar{I}| = \epsilon$. Thus, the cut off τ_1 obeys an equation of a vertical line $\tau_1 = t_c$.

Notice that there are two different definitions for τ_1 . Each one corresponds to a particular sub-regions A ($x \rightarrow \infty$) or B ($x \rightarrow 0$). Consequently, the truncation τ_1 for the trans-stable function is defined by two equations which depend on the x and ϵ values. These two equations have their intersection point at (t_c, x_c) :

$$\tau_1(\epsilon, x) = \begin{cases} t_c(\epsilon) & \text{if } x > x_c \\ x/\alpha & \text{if } x < x_c \end{cases} \text{ for } \alpha > 1, \quad (35)$$

where $t_c(\epsilon)$ and x_c are given by the implicit form of the

following equations:

$$\begin{aligned} \alpha t_c^2 + t_c^\alpha \cos(\pi\alpha/2) + \ln(\epsilon) &= 0, \\ x_c &= \alpha t_c. \end{aligned} \quad (36)$$

Figure 4 illustrates the contour plot of the instantaneous amplitude $|\bar{I}|$ for $\alpha = 1.4$. The truncation τ_1 is presented as a cut-off made when a negligible value of instantaneous amplitude is achieved $|\bar{I}| = \epsilon = 10^{-3}$. The point (x_c, t_c) is located at the intersection between the contour line of the given tolerance ϵ and the equation $\tau_1 = x/\alpha$. The truncation τ_1 avoids zone B which contains negative values for \bar{g} with $\partial g / \partial t > 0$. One can observe that there is an abrupt upward trend in $|\bar{I}|$ for $x \rightarrow 0$. So, the truncation τ_1 allows us to make a perfect cut off before this upward trend starts. It is noticeable that with a small tolerance ϵ the intersection will occur in the rightmost part of the figure, consequently the interval of integration will be wider and a more accurate result can be obtained.

Figure 5 shows how the solutions of trans-stable and Lévy-stable distribution functions are quite similar after x_c value, which depends on the tolerance ϵ . For a smaller ϵ the similarity of both asymptotic series is expected to improve due to a wider interval of integration. However, the value x_c will be higher and the similarity will start at the rightmost part of the axis.

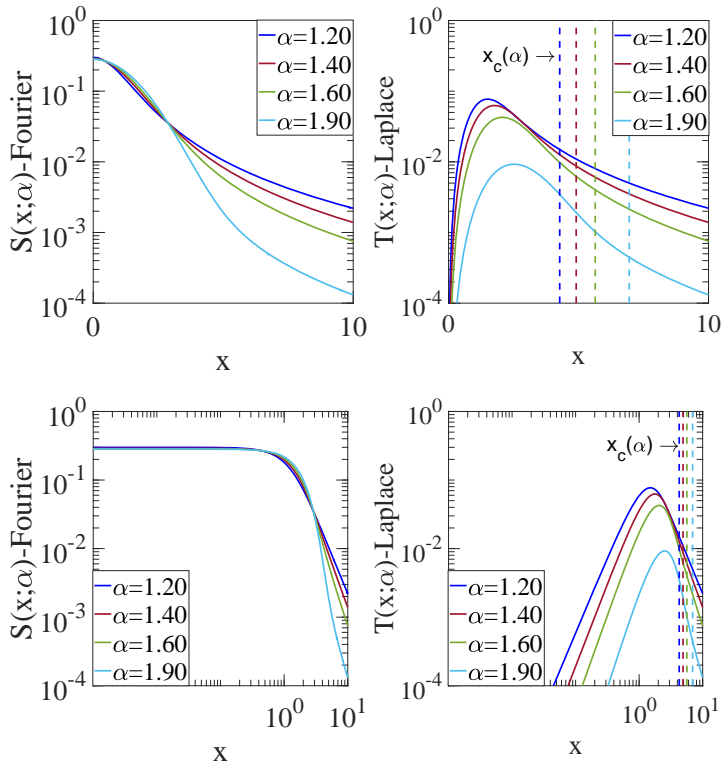


Figure 5. Comparison of numerical integration $1 < \alpha < 2$ between Fourier and Laplace transform of Lévy-stable $S(x; \alpha)$ and trans-stable $T(x; \alpha)$ functions using recursive adaptive Simpson quadrature method [59]. The absolute error tolerance of the method is $\xi = 3.5 \times 10^{-8}$. Top plots are shown in semi-logarithmic scale and in logarithmic scale.

V. ASYMPTOTIC EXPANSIONS

Asymptotic expansions are developed to obtain closed-form representations for the Lévy-stable distribution function $S(x, \alpha)$. These expansions are based on the Taylor series of the complex exponential function,

$$e^z \sim \sum_{k=0}^n \frac{z^k}{k!} \quad \text{as } n \rightarrow \infty. \quad (37)$$

Two different asymptotic expansions will be performed. The first one corresponds to the ‘inner expansion’. To get this solution the Lévy-stable distribution function is evaluated by expanding e^{ixt} of Eq. (15) and (26) around $x = 0$. The second one refers to the ‘outer expansion’, which is the asymptotic series expansion for $x \rightarrow \infty$. When $x \gg 1$, the oscillations of the integrands in Eq. (15) and (26) are large. Consequently, there are important cancellations due to factor e^{ixt} in the integral. Thus, we focus our integration in the region with the major contribution in the integral, that is around $t = 0$. In consequence, the amplitude of the integral $e^{t\alpha}$ is replaced by its Taylor expansion around $t = 0$. To guarantee the convergence of the series expansion, the improper integrals are truncated. The truncation occurs because of the sufficient conditions for Riemann integral existence.

These conditions are that the integrand must be bounded and the domain of integration is a closed interval [60, 61].

A. Inner Expansion

The inner expansion is obtained making a substitution of e^{ixt} by its Taylor series expansion given by Eq. (37) in the integrand of the Lévy-stable distribution I . After this substitution, the integrals in Eq. (15) and (26) can be analytically solved. The difference between these two equations are the truncation on the interval of integration.

For $\alpha \leq 1$ the convergence of the series is slow, demanding a large value of order n in Eq. (37) to reach an acceptable similarity with the original integrand I . For this reason, the improper integral is truncated after a small enough amplitude of I is obtained. For $\alpha > 1$ the convergence occurs faster and truncation is not needed.

1. For $0 < \alpha \leq 1$

The inner expansion is obtained by substituting e^{ixt} in Eq. (26) by its Taylor expansion using Eq. (37). Then:

$$S_i(x; \alpha, \epsilon) = \frac{1}{\pi} \int_0^{\tau_2(x, \epsilon)} e^{-t^\alpha} e^{ixt} dt \sim \frac{1}{\pi} \int_0^{\tau_2(x, \epsilon)} I_n dt \quad \text{as } n \rightarrow \infty, \quad (38)$$

where I_n is given by:

$$I_n(x; t, \alpha) = \sum_{k=0}^n e^{-t^\alpha} \frac{(ixt)^k}{k!}. \quad (39)$$

The upper limit τ_2 is given by the following equation:

$$\tau_2(x, \epsilon) = -\frac{\ln(\epsilon)}{x}. \quad (40)$$

This truncation results from the equation $e^{ix\tau_2} = \epsilon$, where ϵ represents the tolerance that needs to be small to ensure a cut-off when negligible quantities of $|I|$ and $|I_n|$ are obtained. Consequently, the area under the curve of both functions are similar.

The convergence of I_n to I demands a large value of order n in Eq. (37), as it can be observed in Fig (6). This occurs because of slow decay of e^{-t^α} value for $\alpha < 1$. This is the reason to evaluate the integral in the closed interval $[0, \tau_2]$, where the original integrand I and its Taylor series approximation I_n are similar.

The integrals in Eq. (38) can be solved without difficulty. Then, the inner expansion s_i is given by the real part of this solution,

$$s_i(x; \alpha, \epsilon) = \text{Re}(S_i(x; \alpha, \epsilon)).$$

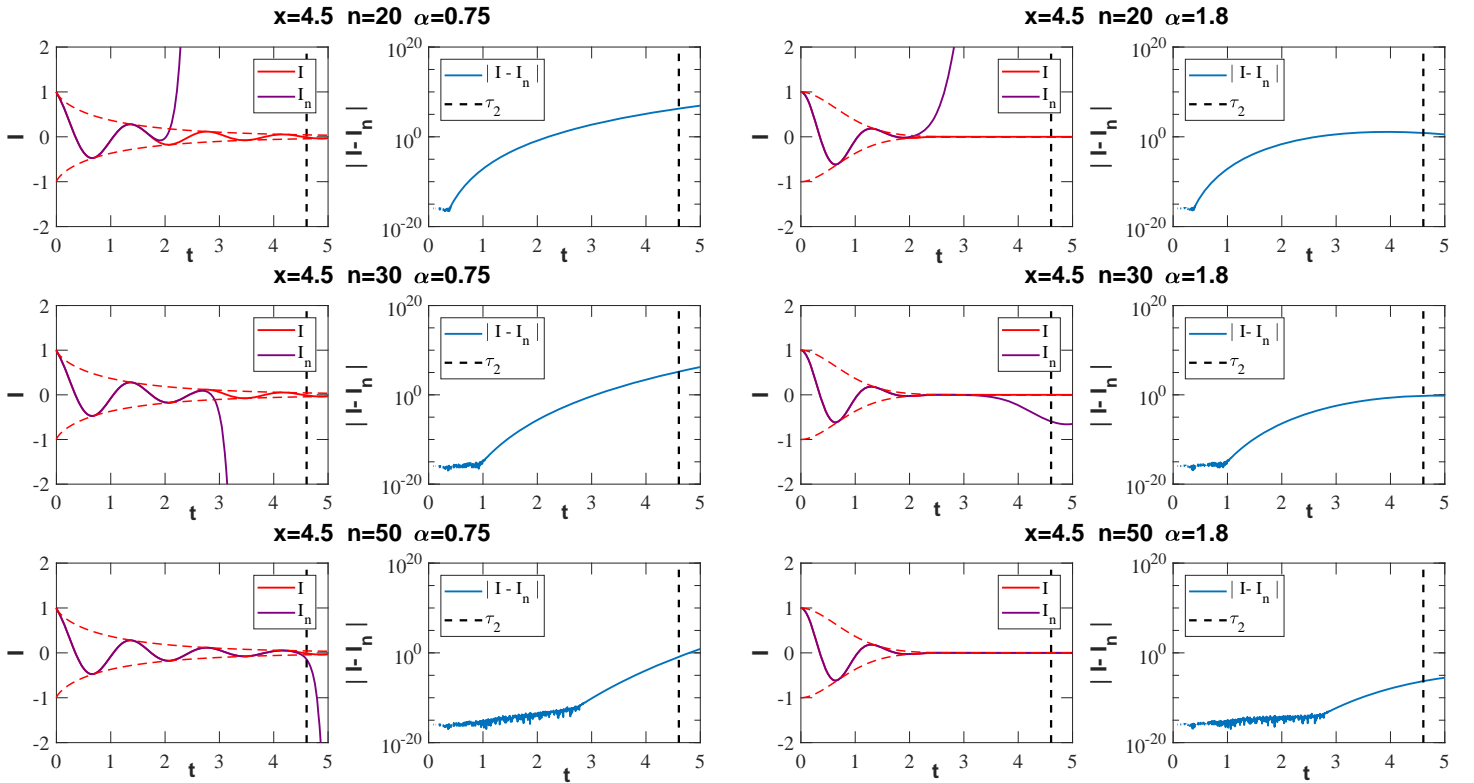


Figure 6. Comparison of $I = e^{t^\alpha} e^{ixt}$ and $I_n = e^{t^\alpha} \sum_{k=0}^n \frac{(ixt)^k}{k!}$ of Eq. (38) and (43), where I_n is obtained by replacing e^{ixt} in I by its Taylor expansion. The plots are for $\alpha = 0.75$ (left) and $\alpha = 1.8$ (right). For $\alpha \leq 1$, the truncation is required to ensure a cut-off when negligible quantities of $|I|$ and $|I_n|$ are obtained. The truncated error of the Taylor expansion is measured by using the absolute value of the difference $|I - I_n|$. For $\alpha > 1$, since the convergence is fast the truncation is unnecessary. For these particular examples, the integrand I is evaluated at $x = 4.5$ for three cases of $n = 20, 30, 50$ with $\epsilon = 10^{-9}$.

Consequently,

$$s_i(x; \alpha, \epsilon) = \frac{1}{\pi\alpha} \sum_{k=0}^{\infty} \frac{x^k}{k!} \gamma\left(\frac{k+1}{\alpha}, \tau_2(x; \epsilon)^\alpha\right) \cos\left(\frac{\pi k}{2}\right), \quad (41)$$

where γ represents the incomplete gamma function [62],

$$\gamma(z, b) = \int_0^b x^{z-1} e^{-x} dx. \quad (42)$$

Due to a computation of the incomplete gamma function γ , Eq. (41) was modified for numerical analysis in Matlab² [63].

²Note: Matlab defines the incomplete gamma function as γ^*

$$\gamma^*(b, z) = \frac{1}{\Gamma(z)} \int_0^b x^{z-1} e^{-x} dx$$

where $\Gamma(z)$ is the gamma function.

2. For $1 < \alpha < 2$

Here it is derived the inner expansion s_i for $\alpha > 1$ from the non-truncated form of Lévy-stable distribution function. This derivation is made by substituting e^{ixt} in Eq. (15) by its Taylor expansion in Eq. (37), then:

$$S_i(x; \alpha) = \frac{1}{\pi} \int_0^\infty e^{-t^\alpha} e^{ixt} dt \sim \frac{1}{\pi} \int_0^\infty I_n dt \quad \text{as } n \rightarrow \infty. \quad (43)$$

For $\alpha > 1$, the convergence of integrand I and the integrand after the substitution I_n occurs faster than for $\alpha < 1$. This feature is observed in Figure (6), where an acceptable convergence between I and I_n is obtained with a small n value. Consequently, the integral is evaluated without truncation or taking the limit $\epsilon \rightarrow 0$ in Eq. (38).

Then, it is only considered the real part of the solution of Eq. (43),

$$s_i(x; \alpha) = \text{Re}(S_i(x; \alpha)).$$

Consequently,

$$s_i(x; \alpha) = \frac{1}{\pi\alpha} \sum_{k=0}^{\infty} \frac{x^k}{k!} \Gamma\left(\frac{k+1}{\alpha}\right) \cos\left(\frac{\pi k}{2}\right), \quad (44)$$

where Γ represents the gamma function [62],

$$\Gamma(b) = \int_0^{\infty} x^{b-1} e^{-x} dx.$$

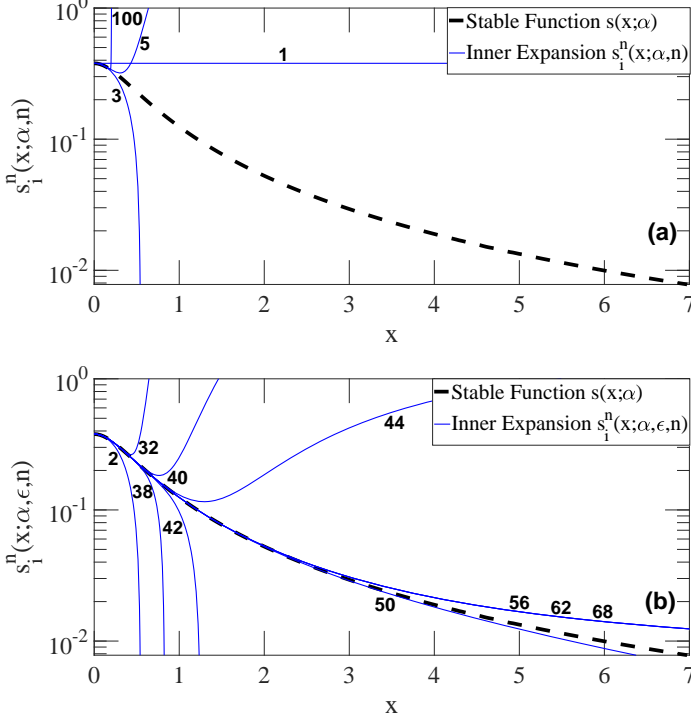


Figure 7. Inner expansion of the Lévy-stable distribution function for $\alpha = 0.75$. This is obtained by applying Taylor expansion around $t = 0$. The subfigure (a) is a non-truncated integral. The subfigure (b) is the truncated integral with tolerance $\epsilon = 10^{-9}$ in Eq. (41), which displays a fast convergence due to integral's truncation.

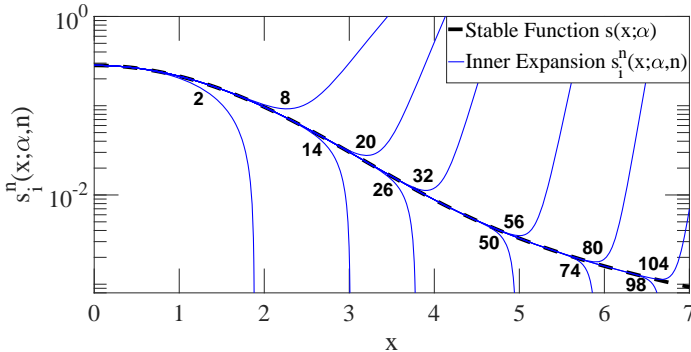


Figure 8. Inner expansion of the Lévy-stable distribution for $\alpha = 1.80$ as a result of applying a Taylor expansion in the ‘exponential of the phase’ of the integrand. The figure illustrates the non-truncated Lévy-stable solution in Eq. (44). This figure displays a fast convergence so that no truncation is needed.

Examples for $\alpha = 0.75$ and $\alpha = 1.80$ are shown on Figures 7 and 8 respectively. In Figure 7, for $\alpha \leq 1$ the truncation τ_2 is needed, otherwise the convergence to Lévy-stable distribution function will be ultraslow as $n \rightarrow \infty$. This is evident when a comparison is made between subfigure 7a and 7b. They represent a non-truncated and truncated Lévy-stable solution respectively. The subfigure 7b displays an acceptable convergence with a smaller order n . In Figure 8, for $\alpha > 1$ the convergence to the Lévy-stable distribution function occurs faster and no truncation is needed. For both cases the inner expansion s_i behaves well because it converges to $s(x; \alpha)$.

B. Outer Expansion

The outer expansion is obtained making a substitution of the amplitude e^{-t^α} in the integrand of the truncated Lévy-stable distribution function I in Eq. (26) by its Taylor series expansion around $t = 0$. Then, the following relation is obtained:

$$S_o(x; \alpha, \epsilon) = \frac{1}{\pi} \int_0^{\tau_3(\epsilon)} e^{-t^\alpha} e^{ixt} dt \sim \frac{1}{\pi} \int_0^{\tau_3(\epsilon)} G_n dt \quad \text{as } n \rightarrow \infty, \quad (45)$$

where G_n is given by:

$$G_n(x; \alpha) = \sum_{k=0}^n \frac{(-t^\alpha)^k}{k!} e^{ixt}. \quad (46)$$

The upper limit τ_3 is given by the following equation:

$$\tau_3(\epsilon) = [-\ln(\epsilon)]^{1/\alpha}. \quad (47)$$

This truncation is calculated from $e^{-\tau_3^\alpha} = \epsilon$, where ϵ is defined as tolerance and represents a negligible instantaneous amplitude when ϵ is small. The truncation allows a faster convergence of G_n to I and reduces the error of integration due to an accurate approximation on the interval $[0, \tau_3]$.

The original integrand I and the new integrand after applying Taylor series G_n in Eq. (45) were evaluated in Figure 9. Since the convergence of G_n to I is slow, the truncation τ_3 is considered to define the new interval of integration $[0, \tau_3]$.

To obtain the outer solution s_o a change of variable after the series expansion is applied in Eq. (45). The change of variable is $-u = ixt$, so $-du = ixdx$. This gives us an approximation of the form:

$$S_o(x; \alpha, \epsilon) \sim \frac{1}{\pi} \sum_{k=0}^n \frac{(-1)^k}{k!} \left(\frac{-1}{ix}\right)^{k\alpha+1} \int_0^{-ix\tau_3(\epsilon)} u^{k\alpha} e^{-u} du. \quad (48)$$

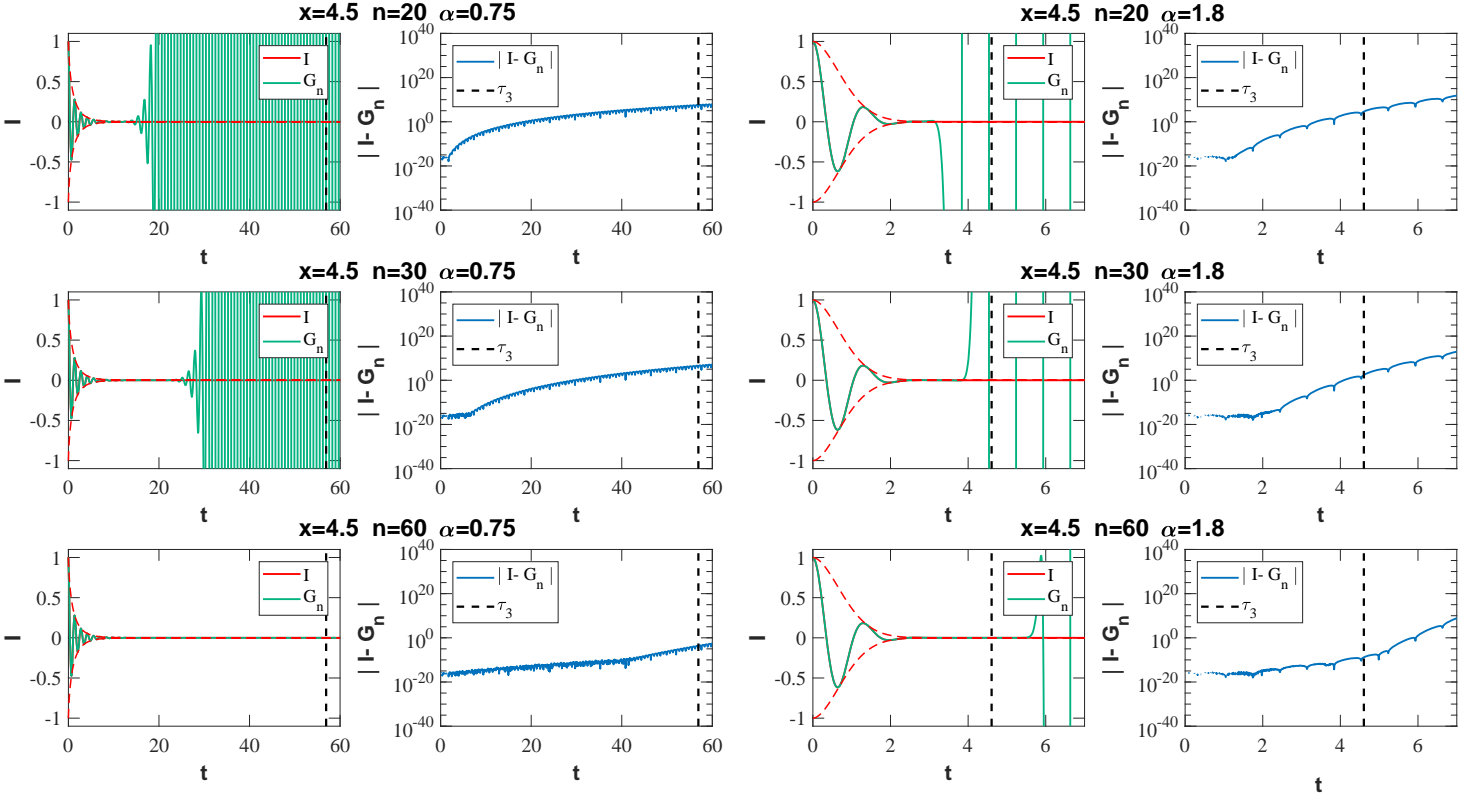


Figure 9. Comparison of $I = e^{t^\alpha} e^{ixt}$ and $G_n = \frac{(-t^\alpha)^k}{k!} e^{ixt} dt$ of Eq. (45), where G_n is the Taylor expansion of I around $t = 0$. The plots correspond to $\alpha = 0.75$ (left) and $\alpha = 1.8$ (right). Truncation of the integral is required for both cases. The reason of that is to reach an accurate approximation between the original integrand I and the one after the series expansion G_n . The error is measured by the absolute value of the difference $|I - G_n|$. For these particular examples, the integrand I is evaluated at $x = 4.5$ for three cases of $n = 20, 30, 50$ with $\epsilon = 10^{-9}$.

To solve the integral, the incomplete gamma function of imaginary argument $\gamma(v, iz)$ is used [62, 64]. The following solution is presented by Barak as a special case of confluent hypergeometric function [64],

$$\begin{aligned} \gamma(v, iz) &= \int_0^{iz} t^{v-1} e^{-t} dt \\ &= (iz)^v v^{-1} {}_1F_1(v, 1+v, -iz), \end{aligned} \quad (49)$$

where ${}_1F_1(v, 1+v, -iz)$ represents the Confluent Hypergeometric function. Then, comparing Eq. (48) and (49), we obtain the following relation between the variables, $v = k\alpha + 1$, $z = -x\tau_3$ and $t = u$.

Finally, the real part of the solution is:

$$s_o(x; \alpha, \epsilon) = \text{Re}(S_o(x; \alpha, \epsilon)).$$

Consequently,

$$\begin{aligned} s_o(x; \alpha, \epsilon) &= -\frac{1}{\pi} \sum_{k=1}^{\infty} \frac{(-1)^k}{k!} \left(\frac{\cos(\pi\alpha k)}{k\alpha + 1} \right) \dots \\ &\dots (-\tau_3(\epsilon))^{k\alpha+1} {}_1F_1(k\alpha + 1, k\alpha + 2, ix\tau_3(\epsilon)). \end{aligned} \quad (50)$$

Figure 10 shows the calculation of Eq. 50 for $\alpha = 1.8$. In this figure is evident that the outer expansion s_o converges slowly. This occurs due to computation of the confluent hypergeometric function ${}_1F_1$ which demands considerable computational time. The series that define the function ${}_1F_1$ do not have a trivial structure, this creates numerical issues which makes the calculation computational inefficient [65]. The approximation in Figure 10 shows how the convergence demands a large value of order n to obtain an accurate approximation at the tail. The convergence resembles waves that slowly start to decrease from the tails to the peak of Lévy-stable distribution. The series until $n = 30$ does not show an acceptable approximation. Only an approximation on tails are obtained after $n = 40$. For $x \rightarrow 0$, the series of s_o converges to a specific value different of the Lévy-stable distribution function. The convergence to the Lévy-stable distribution function is observed only for $x \rightarrow \infty$.

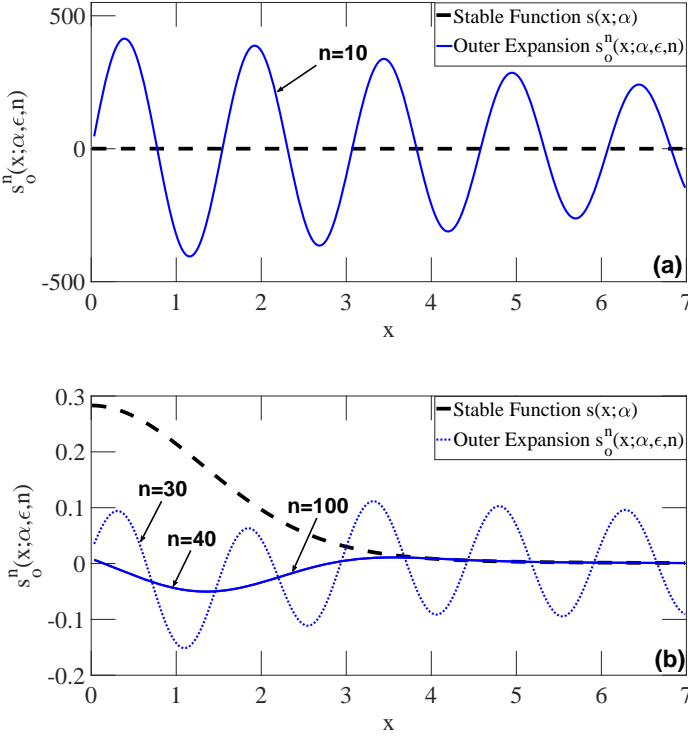


Figure 10. Outer expansion s_o for $\alpha = 1.80$ with tolerance $\epsilon = 10^{-6}$ in Eq. (50). The subfigure (a) and (b) correspond to $n = 10, 30, 40, 100$ respectively.

C. Outer expansion by Trans-Stable distribution

Because of the slow convergence of the outer expansion s_o and its wave-like behaviour, an alternative approximation is obtained using the trans-stable function $T(x; \alpha)$. As it was previously explained in section IV, the solutions of trans-stable $T(x; \alpha)$ and Lévy-stable $S(x; \alpha)$ functions are identical for $0 < \alpha \leq 1$ and similar for $1 < \alpha < 2$ after the x_c value. Consequently, the improper integral in Eq. (24) is used to calculate the series expansions for $0 < \alpha \leq 1$ and the truncated trans-stable integral in its Laplace representation in Eq. (29) for $1 < \alpha < 2$.

This outer expansion t_o is given by the analytical solution of the trans-stable function after applying the Taylor series of $e^{-(it)^\alpha}$ around $t = 0$ in the trans-stable integrand \bar{I} using Eq. (37) and (24). Then, the following equation is shown:

$$T_o(x; \alpha, \epsilon) = \frac{1}{\pi} \int_0^{\tau_1(x, \epsilon)} e^{-(it)^\alpha} e^{-xt} i dt \sim \frac{1}{\pi} \int_0^{\tau_1(x, \epsilon)} K_n dt, \quad (51)$$

where K_n is given by:

$$K_n(x) = \sum_{k=0}^n \frac{(-it)^\alpha{}^k}{k!} e^{-xt} i. \quad (52)$$

Due to a slow convergence of K_n to \bar{I} the cut-off τ_1 is applied. The truncation τ_1 has two different expressions. For $\alpha \leq 1$, the truncation τ_1 depends on the tolerance ϵ and for $\alpha > 1$ it depends on the tolerance ϵ and x values. These expressions will be explained in the following subsections.

To solve the integral in Eq. (51), the following change of variable is applied: $xt = u$ and $x dt = du$. This leads to the following series expansion:

$$T_o(x; \alpha, \epsilon) \sim \frac{1}{\pi} \sum_{k=0}^{\infty} \frac{(-1)^k}{k!} \left(\frac{-1}{ix}\right)^{k\alpha+1} \int_0^{x\tau_1(x, \epsilon)} u^{(k\alpha+1)-1} e^{-u} du. \quad (53)$$

The upper limit of the integral changes from τ_1 to $x\tau_1$, but still remains on the real axis. The integral above can be solved using the incomplete gamma function defined in Eq. (42). Then, the real part of the result is obtained,

$$t_o(x; \alpha, \epsilon) = \text{Re}(T_o(x; \alpha, \epsilon)).$$

Consequently,

$$t_o(x; \alpha, \epsilon) = -\frac{1}{\pi} \sum_{k=1}^{\infty} \frac{(-1)^k}{k!} \left(\frac{1}{x}\right)^{k\alpha+1} \sin\left(\frac{\pi\alpha k}{2}\right) \gamma(k\alpha + 1, x\tau_1(x, \epsilon)). \quad (54)$$

The determination of τ_1 for $\alpha \leq 1$ and $\alpha > 1$ is presented in the following subsections.

1. For $0 < \alpha \leq 1$

For $\alpha \leq 1$, the cut-off τ_1 in Eq. (54) is given by the following equation:

$$\tau_1(\epsilon) = [-\ln(\epsilon)]^{1/\alpha} \quad \text{for } \alpha \leq 1. \quad (55)$$

This truncation is obtained from $e^{-\tau_1^\alpha} = \epsilon$, where the tolerance ϵ represents a negligible instantaneous amplitude for the integrands in Eq. (51).

2. For $1 < \alpha < 2$

The truncation τ_1 in Eq. (54) for $1 < \alpha < 2$ was already obtained in subsection IV-2 and defined by Eq. (35) as:

$$\tau_1(x, \epsilon) = \begin{cases} t_c(\epsilon) & \text{if } x > x_c, \\ x/\alpha & \text{if } x < x_c, \end{cases} \quad \text{for } \alpha > 1,$$

where t_c and x_c were defined by Eq. (36). As indicated in subsection IV-2, the value of τ_1 is used to minimize the truncation error and at the same time to make the domain of integration as small as possible.

The outer expansion by the trans-stable function converges to the original trans-stable function. Examples are shown in Figure 11 for $\alpha \leq 1$ and Figure 12 for $\alpha > 1$. Note that in both cases the truncation τ_1 allows a faster and more accurate convergence to the real part of the trans-stable distribution $t(x; \alpha)$. Consequently the outer solution t_o shows an identical solution as $s(x; \alpha)$ for $\alpha \leq 1$ and the same asymptotic behaviour for $\alpha > 1$. For a smaller ϵ the convergence of these outer expansions to the trans-stable function will occur faster. Also in Figure 11 the non-truncated trans-stable expansion is shown as an expansion that converges extremely slowly requiring a higher order n than truncated trans-stable expansion to obtain an acceptable convergence. In Figure 12 the non-truncated trans-stable expansion does not converge to trans-stable function at all.

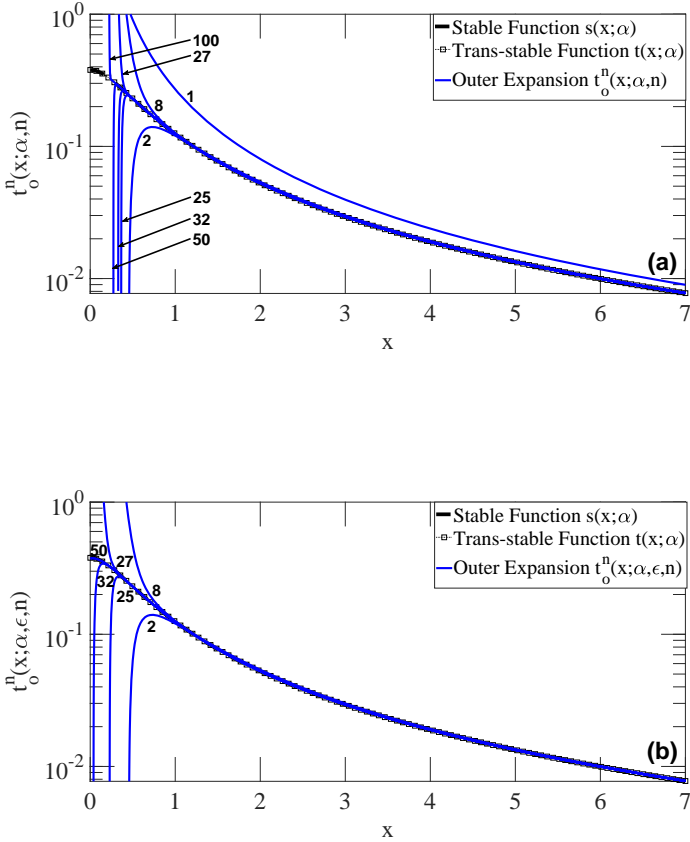


Figure 11. Outer expansion of the trans-stable function for $\alpha = 0.75$. This result is obtained from the Taylor expansion of the integrand around $t = 0$ in Eq. (54) and (55). The subfigure (a) is the non-truncated integral that shows slow convergence. The subfigure (b) corresponds to truncated integral with tolerance $\epsilon = 10^{-6}$. The subfigure (b) displays a faster convergence to the trans-stable function as a result of the truncation of the integral.

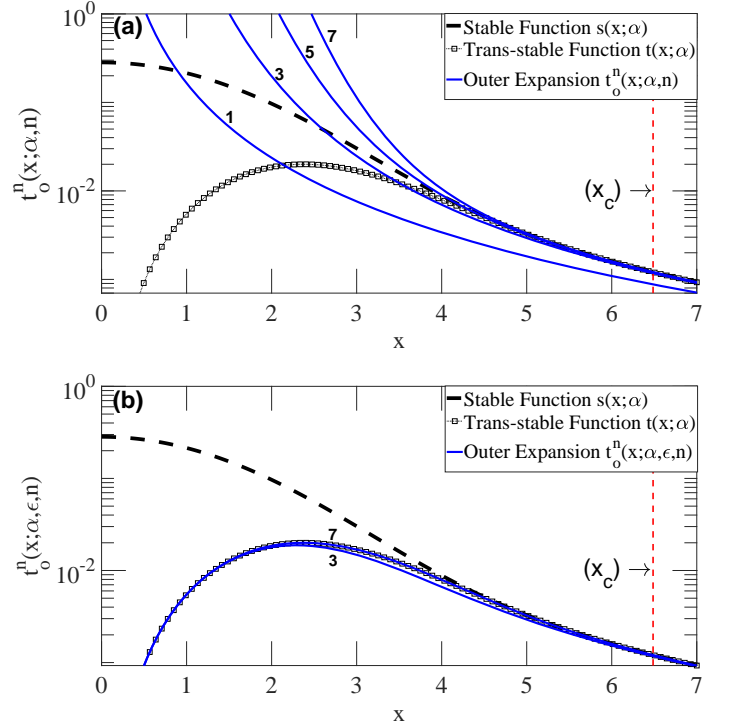


Figure 12. Outer expansion of the trans-stable for $\alpha = 1.80$ as a result of applying Taylor expansion of the integrand around $t = 0$ in Eq. (35) and (54). The subfigure (a) shows that the non-truncated integral does not converge to the trans-stable function. The subfigure (b) corresponds to the truncated integral with tolerance $\epsilon = 10^{-6}$. The subfigure (b) displays a fast convergence as a result of the truncation of the integral.

VI. UNIFORM SOLUTION

The uniform solution is presented as the combination of the inner solution and the outer solution to construct an approximation valid for all $x \in [-\infty, \infty]$. To construct the uniform solution an asymptotic matching method based on boundary-layer theory is applied [66, 67]. This method is based on superposing the inner and outer solution and subtracting the overlap between them,

$$s_u(x) = y_{out}(x) + y_{in}(x) - y_{overlap}(x). \quad (56)$$

The overlap is defined as the limit of the rightmost edge of y_{in} and the leftmost edge of y_{out} ,

$$y_{overlap} = \lim_{x \rightarrow 0} y_{out} = \lim_{x \rightarrow \infty} y_{in}. \quad (57)$$

For this case, our proposed uniform solution s_u is constructed based on our inner expansion s_i and our outer expansion t_o . These previous solutions were already defined in section V.

For a better understanding of our uniform solution s_u , two sub-sections A and B are presented. Sub-section A

Range of α	$0 < \alpha \leq 1$	$1 < \alpha < 2$
Normalized Lévy-stable distribution (s)	$s(x; \alpha) = \frac{1}{\pi} \int_0^{\infty} e^{-t^\alpha} \cos(tx) dt$	
Normalized trans-stable distribution (t)	$t(x; \alpha) = \frac{1}{\pi} \int_0^{\infty} e^{-t^\alpha \cos(\frac{\pi\alpha}{2}) - xt} \sin(t^\alpha \sin(\frac{\pi\alpha}{2})) dt$	
Inner expansion (s_i^n)	$s_i^n(x; \alpha, \epsilon) = \frac{1}{\pi\alpha} \sum_{k=0}^n \frac{x^k}{k!} \gamma\left(\frac{k+1}{\alpha}, \tau_2^\alpha\right) \cos\left(\frac{\pi k}{2}\right)$ $\tau_2 = \frac{-\ln(\epsilon)}{x}$	$s_i^n(x; \alpha) = \frac{1}{\pi\alpha} \sum_{k=0}^n \frac{x^k}{k!} \Gamma\left(\frac{k+1}{\alpha}\right) \cos\left(\frac{\pi k}{2}\right)$
Outer expansion (s_o^n)	$s_o^n(x; \alpha, \epsilon) = -\frac{1}{\pi} \sum_{k=1}^n \frac{(-1)^k}{k!} \left(\frac{\cos(\pi\alpha k)}{k\alpha + 1}\right) (-\tau_3)^{k\alpha+1} {}_1F_1(k\alpha + 1, k\alpha + 2, ix\tau_3)$ $\tau_3 = [-\ln(\epsilon)]^{1/\alpha}$	
Outer solution ³ (t_o^n)	$t_o^n(x; \alpha, \epsilon) = -\frac{1}{\pi} \sum_{k=1}^n \frac{(-1)^k}{k!} \left(\frac{1}{x}\right)^{k\alpha+1} \gamma(k\alpha + 1, x\tau_1) \sin\left(\frac{\pi\alpha k}{2}\right)$	
	$\tau_1 = (-\ln(\epsilon))^{1/\alpha}$	$\tau_1 = \begin{cases} t_c & \text{if } x > x_c \\ x/\alpha & \text{if } x < x_c \end{cases}$
Complete and incomplete gamma functions (Γ) & (γ)	$\Gamma(z) = \int_0^{\infty} x^{z-1} e^{-x} dx$ $\gamma(z, b) = \int_0^b x^{z-1} e^{-x} dx$	

Table II. Summary of Inner and Outer Solutions

contains a summary of inner and outer expansions previously obtained. In sub-section B the steps taken to obtain s_u are explained.

A. Summary of inner and outer expansions

Table II contains the normalized Lévy-stable and trans-stable distribution and the summary of previous results obtained from Lévy-stable and trans-stable functions by applying Taylor expansions. The series refers to one inner expansion s_i and two outer expansions s_o and t_o .

For the inner expansion s_i , the solution for $\alpha \leq 1$ corresponds to a truncated Lévy-stable solution which allows a faster convergence. For $\alpha > 1$ the series is obtained from the non-truncated Lévy-stable solution. The only difference between them is the use of the incomplete gamma function γ in the solution for $\alpha \leq 1$, where $\Gamma(z) = \lim_{b \rightarrow \infty} \gamma(z, b)$. Consequently, for both cases the truncated series can provide a good approximation. However, in the case of $\alpha \leq 1$ we must take the limit as:

$$s(x; \alpha) = \lim_{\epsilon \rightarrow 0} \left(\lim_{n \rightarrow \infty} s_i^n(x; \alpha, \epsilon) \right) \quad \text{for } x < \infty.$$

In general the order how we apply the limits cannot be exchanged. However, in the case of $\alpha > 1$ the order of the limits does not affect the convergence. Taking a small value of ϵ ensures a faster convergence.

For the outer expansion two expressions were derived.

³Note: Refer to equation Eq. (35) to obtain t_c and x_c value for $1 < \alpha < 2$

The first outer expansion s_o is obtained by performing the Taylor expansion around $t = 0$ on the truncated Lévy-stable distribution. This solution displays a slow convergence for $n \rightarrow \infty$. The second outer expansion t_o is obtained by applying the Taylor expansion on the truncated trans-stable function for $x \rightarrow \infty$. The truncation of t_o depends on α and there are two different cases. For $\alpha \leq 1$ it converges to the exact solution of $s(x; \alpha)$ and for $\alpha > 1$ it converges to the same solution at the tails of $s(x; \alpha)$. To guarantee convergence, we need to take the limit as,

$$t(x; \alpha) = \lim_{\epsilon \rightarrow 0} \left(\lim_{n \rightarrow \infty} t_o^n(x; \alpha, \epsilon) \right) \quad \text{for } x > 0.$$

Exchanging the order of the limits will affect the convergence. The outer expansion that will be used is t_o , because it displays a faster convergence and it does not exhibit wavelike behaviour.

B. Steps to obtain the uniform solution

To obtain the uniform solution s_u the condition in Eq. (57) needs to be satisfied. The inner expansion s_i and the outer expansion t_o have to be multiplied with an appropriate coefficient $A(x)$ to obtain the asymptotic solutions with a common matching value y_m . These operations will allow us to obtain y_{out} and y_{in} . Consequently, Eq. (56) will be applied to obtain the closed-form solution of the Lévy-stable distribution function.

Below the steps are explained to obtain the location of the matching between the inner and the outer solutions (x_m, y_m) , the coefficient $A(x)$, and the uniform solution s_u .

1. Finding inner and outer limit (x_m, y_m)

Considering s_i and t_o as good approximations to the Lévy-stable distribution function, we must require that the inner and the outer expansions will be close enough before matching them [68]. Consequently, the point where the matching between s_i and t_o takes place is (x_m, y_m) and it represents the location where the minimal vertical distance between the inner s_i and the outer solution t_o occurs.

The distance function between s_i and s is defined as δ_i and the distance function between t_o and s is δ_o . Consequently, (x_m, y_m) is the point where the Pythagorean addition of these distances is minimal Eq. (58):

$$\delta_i^2(x; \alpha, \epsilon) = (s(x; \alpha) - s_i(x; \alpha, \epsilon))^2,$$

$$\delta_o^2(x; \alpha, \epsilon) = (s(x; \alpha) - t_o(x; \alpha, \epsilon))^2,$$

$$\delta^2(x; \alpha, \epsilon) = \delta_o^2(x; \alpha, \epsilon) + \delta_i^2(x; \alpha, \epsilon),$$

$$\left. \frac{d(\delta^2(x; \alpha, \epsilon))}{dx} \right|_{x_m} = 0. \quad (58)$$

The x_m value is obtained from the previous equation. Then, y_m is defined by the equidistant point between both functions,

$$y_m = \frac{s_i(x_m) + t_o(x_m)}{2}. \quad (59)$$

2. Defining the inner and the outer solutions y_{in} and y_{out}

To obtain the uniform solution s_u , the asymptotic matching method based on boundary layer theorem [66] is applied. Consequently, the inner solution y_{in} and the outer solution y_{out} must have a matching asymptotic behaviour. More precisely, the limit of the outer solution y_{out} when $x \rightarrow 0$ should correspond to the limit of the inner solution y_{in} when $x \rightarrow \infty$. To obtain y_{in} and y_{out} solutions, the series expansions s_i and t_o are multiplied by an appropriate coefficients to meet the requirements of matching asymptotic expansions, so the y_{in} and y_{out} are defined as follows:

$$y_{in}(x; \alpha, \epsilon, \mu) = (s_i(x) - y_m)(1 - A(x; \mu)) + y_m, \quad (60)$$

$$y_{out}(x; \alpha, \epsilon, \mu) = (t_o(x) - y_m)A(x; \mu) + y_m, \quad (61)$$

where the overlapping factor $A(x)$ is defined as:

$$A(x; \mu) = \frac{1}{2} \left(1 + \tanh \left(\frac{x - x_m}{\mu} \right) \right). \quad (62)$$

The $A(x; \mu)$ is used to smooth s_i and t_o and provides them with a symmetric overlap section around x_m and gives y_{in} and y_{out} an asymptotic behaviour. The variable μ determines the width of the overlap between y_{in} and y_{out} .

It is easy to see that Eq. (60) and Eq. (61) satisfy Eq. (57), where the limits of y_{out} and y_{in} converge to a constant value y_m .

3. Defining the Uniform Solution s_u

The inner solution y_{in} Eq. (60) and the outer solution y_{out} in Eq. (61) were defined to fulfill the requirements for matching asymptotic expansions. Then, Eq.(56) is applied to obtain the uniform solution s_u ,

$$s_u^{n_i, n_o}(x; \alpha, \epsilon, \mu) = \frac{t_o^{n_o}(x; \alpha, \epsilon)}{2} + \frac{s_i^{n_i}(x; \alpha, \epsilon)}{2} \dots \\ \dots + \tanh \left(\frac{x - x_m}{\mu} \right) \left(\frac{t_o^{n_o}(x; \alpha, \epsilon)}{2} - \frac{s_i^{n_i}(x; \alpha, \epsilon)}{2} \right). \quad (63)$$

4. Find the best s_u by choosing the most appropriate μ

The width of the overlap between y_{in} and y_{out} can be optimized to obtain the closest solution s_u of the Lévy-stable distribution function. The most appropriate value of μ needs to be obtained for each particular value of α . For that, the least square method will be applied between the original $s(x; \alpha)$ and the new closest solution $s_u(x; \alpha, \epsilon, \mu)$. Applying Eq. (12) and (63) the following equation is obtained:

$$L(\mu) = \sum_{i=1}^N (s_u(x_i; \alpha, \epsilon, \mu) - s(x_i; \alpha))^2, \quad (64)$$

where the N value represents the length of the sample used to minimize L .

The similarity between the exact solution of $s(x; \alpha)$ and the uniform solution $s_u(x; \alpha, \epsilon, \mu)$ is observed in Figure 13 and 14 for $\alpha = 0.75$ and $\alpha = 1.80$ respectively. For $\alpha < 1$, a good approximation between $s(x; \alpha)$ and $s_u(x; \alpha, \epsilon, \mu)$ is obtained in the tails after mixing two different orders. The order for the inner solution is $n_i = 6$, which makes the solution concave upward. The order for the outer solution is $n_o = 17$, which makes the solution concave downward. This combination of orders will ensure a good matching asymptotic behaviour. For $\alpha > 1$, the uniform solution works well, and a good uniform solution is obtained quickly with a lower order $n = 6$.

Lower orders can be used for both cases, where the most important aspect to consider is the different concavity between y_{in} and y_{out} for the matching asymptotic behaviour. The concavity of the inner and outer solution is defined by the trigonometric element in each solution.

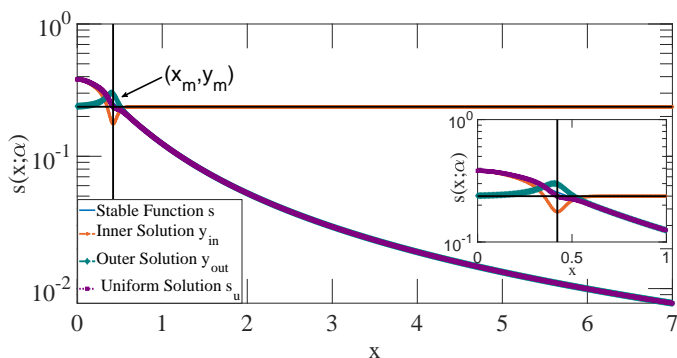


Figure 13. Uniform solution s_u for $\alpha = 0.75$ as a result of joining the inner solution y_{in} with the outer solution y_{out} . The tolerance $\epsilon = 10^{-6}$, $\mu = 0.052$ and $n_i = 6$ and $n_o = 17$.

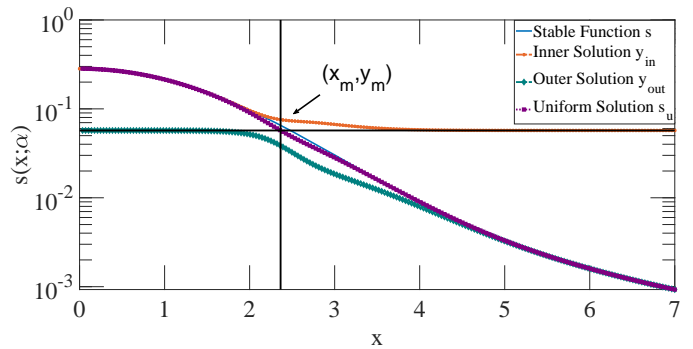


Figure 14. Uniform solution s_u for $\alpha = 1.80$ as a result of joining the inner solution y_{in} with the outer solution y_{out} . The tolerance $\epsilon = 10^{-6}$, $\mu = 0.4$ and $n = 8$.

VII. CONCLUSIONS

In this paper we presented a uniform solution of the Lévy-stable distribution. This solution converges to the Lévy-stable distribution function in the full range of x values $-\infty < x < \infty$. This condition makes our uniform solution more robust than previous analytical expressions that were only applicable for extreme values $x \rightarrow 0$ or $x \rightarrow \infty$. Also, our uniform solution removes the negative values obtained in previous numerical solutions of the Lévy-stable distribution for all α values, which makes this solution more reliable because a probability density function must be always positive.

The uniform solution is the result of an asymptotic matching between the inner and outer expansions. The inner expansion results from the Taylor series expansion of the characteristic function of the Lévy-stable distribution around $x = 0$. The outer expansion is obtained from the Taylor expansion of the integrand of the trans-stable function around $t = 0$. The convergence of these expansions is guaranteed if the integrands are truncated, and the speed of convergence depends on how is the truncation implemented.

For $\alpha \leq 1$, the uniform solution provides a good approximation for all the range of x values. Also, the numerical integration of the trans-stable function constitutes a second option which allows us to obtain a robust numerical solution of the Lévy-stable distribution function and removes the oscillations. For $\alpha > 1$, the uniform solution provides an analytical solution of the Lévy-stable distribution function based on fast converging series. Consequently, the closed-form solution presented in this paper will provide an analytical solution of the fractional kinetic equations (FDE, FDAE, FFPE).

Additionally, having an analytical solution for the Lévy-stable distribution will contribute on modelling stock markets. To achieve this, Lévy-stable noise will be generated numerically. The following procedure is described to generate Lévy-stable noise. First random points between 0 and 1 are generated. Then, the inverse of the cumulative distribution function (CDF) of

the Lévy-stable distribution is applied to these points. Consequently, the corresponding image of the uniformly generated points will be Lévy-stable distributed. Different compromises between accuracy and efficiency in the random number generation can be attained by changing the order n in Eq. (63). Hence, a computational efficiency and high precision are achieved during the generation of large sets of points.

For modelling stock markets, Lévy-stable noise represents the net trading volume —difference between buy and sell stocks' volume— and will feed macroscopic models of the stock markets. On the other hand, to develop microscopic model of stock markets, the Lévy-stable noise can be used to represent the order book (OB)

—list of request for buy and sell orders with prices and volumes—. The use of Levy-Stable noise is justified by the fact that volumes, lifetime of orders, and the placement of limit orders in a OB present power-law decays with coefficients on Lévy-stable range. In consequence, a more realistic microscopic model can be developed by the use of our closed-form solution of the Lévy-stable distribution function.

ACKNOWLEDGMENTS

F. Alonso-Marroquin thanks Hans J. Herrmann for useful discussions and his hospitality in ETHZ.

-
- [1] Donald L Turcotte. Self-organized criticality. *Reports on Progress in Physics*, 62(10):1377, 1999.
 - [2] Bruce D Malamud. Tails of natural hazards. *Physics World*, 17(8):25, 2004.
 - [3] Gennady Samorodnitsky and Murad S. Taqqu. *Stable non-Gaussian random processes: stochastic models with infinite variance*. 1994. ISBN 0412051710;9780412051715;.
 - [4] Parameswaran Gopikrishnan, Vasiliki Plerou, Yan Liu, LA Nunes Amaral, Xavier Gabaix, and H Eugene Stanley. Scaling and correlation in financial time series. *Physica A: Statistical Mechanics and its Applications*, 287(3-4):362–373, 2000.
 - [5] Ofer Biham, Zhi-Feng Huang, Ofer Malcai, and Sorin Solomon. Long-time fluctuations in a dynamical model of stock market indices. *Physical Review E*, 64(2):026101, 2001.
 - [6] Ashadun Nobi, Seong Eun Maeng, Gyeong Gyun Ha, and Jae Woo Lee. Effects of global financial crisis on network structure in a local stock market. *Physica A: Statistical Mechanics and its Applications*, 407:135–143, 2014.
 - [7] Szymon Borak, Wolfgang Hardle, and Rafal Weron. Stable distributions. In *Statistical Tools for Finance and Insurance*, pages 21–44. Springer, 2005.
 - [8] Ying Yuan, Xin-tian Zhuang, Xiu Jin, and Wei-qiang Huang. Stable distribution and long-range correlation of brent crude oil market. *Physica A: Statistical Mechanics and its Applications*, 413:173–179, 2014.
 - [9] Sandro Claudio Lera and Didier Sornette. Gross domestic product growth rates as confined levy flights: Towards a unifying theory of economic growth rate fluctuations. *Physical Review E*, 97(1):012150, 2018.
 - [10] Vasiliki Plerou and H Eugene Stanley. Tests of scaling and universality of the distributions of trade size and share volume: Evidence from three distinct markets. *Physical Review E*, 76(4):046109, 2007.
 - [11] Vasiliki Plerou and H Eugene Stanley. Reply to “comment on ‘tests of scaling and universality of the distributions of trade size and share volume: Evidence from three distinct markets’”. *Physical Review E*, 79(6):068102, 2009.
 - [12] Marcin Magdziarz, Sebastian Orzeł, and Aleksander Weron. Option pricing in subdiffusive bachelier model. *Journal of Statistical Physics*, 145(1):187, 2011.
 - [13] Yoshihiro Yura, Hideki Takayasu, Didier Sornette, and Misako Takayasu. Financial brownian particle in the layered order-book fluid and fluctuation-dissipation relations. *Physical review letters*, 112(9):098703, 2014.
 - [14] Rudolf Friedrich, Joachim Peinke, and Ch Renner. How to quantify deterministic and random influences on the statistics of the foreign exchange market. *Physical Review Letters*, 84(22):5224, 2000.
 - [15] Ralf Metzler, Eli Barkai, and Joseph Klafter. Anomalous diffusion and relaxation close to thermal equilibrium: A fractional fokker-planck equation approach. *Physical review letters*, 82(18):3563, 1999.
 - [16] Ralf Metzler and Joseph Klafter. The random walk's guide to anomalous diffusion: a fractional dynamics approach. *Physics reports*, 339(1):1–77, 2000.
 - [17] Ralf Metzler and Joseph Klafter. The restaurant at the end of the random walk: recent developments in the description of anomalous transport by fractional dynamics. *Journal of Physics A: Mathematical and General*, 37(31):R161, 2004.
 - [18] Rohit Jain and KL Sebastian. Lévy flight with absorption: A model for diffusing diffusivity with long tails. *Physical Review E*, 95(3):032135, 2017.
 - [19] AS Chaves. A fractional diffusion equation to describe lévy flights. *Physica Letters A*, 239(1-2):13–16, 1998.
 - [20] Constantino Tsallis, Silvio VF Levy, André MC Souza, and Roger Maynard. Statistical-mechanical foundation of the ubiquity of lévy distributions in nature. *Physical Review Letters*, 75(20):3589, 1995.
 - [21] Deepika Janakiraman and KL Sebastian. Path-integral formulation for lévy flights: Evaluation of the propagator for free, linear, and harmonic potentials in the over-and underdamped limits. *Physical Review E*, 86(6):061105, 2012.
 - [22] A Kamińska and T Srokowski. Lévy walks in nonhomogeneous environments. *Physical Review E*, 96(3):032105, 2017.
 - [23] Mark M Meerschaert and Charles Tadjeran. Finite difference approximations for fractional advection–dispersion flow equations. *Journal of Computational and Applied Mathematics*, 172(1):65–77, 2004.
 - [24] Tomasz Srokowski. Fractional fokker-planck equation for lévy flights in nonhomogeneous environments. *Physical Review E*, 79(4):04010, 2009.

- [25] Mohsen Ghasemi Nezhadhighi. Scaling characteristics of one-dimensional fractional diffusion processes in the presence of power-law distributed random noise. *Physical Review E*, 96(2):022113, 2017.
- [26] Bartłomiej Dybiec, Ewa Gudowska-Nowak, and Igor M Sokolov. Underdamped stochastic harmonic oscillator driven by lévy noise. *Physical Review E*, 96(4):042118, 2017.
- [27] David A Kessler and Stanislav Burov. Stochastic maps, continuous approximation, and stable distribution. *Physical Review E*, 96(4):042139, 2017.
- [28] VV Yanovsky, AV Chechkin, D Schertzer, and AV Tur. Lévy anomalous diffusion and fractional fokker–planck equation. *Physica A: Statistical Mechanics and its Applications*, 282(1-2):13–34, 2000.
- [29] Carmen Fernandez and Mark FJ Steel. On bayesian modeling of fat tails and skewness. *Journal of the American Statistical Association*, 93(441):359–371, 1998.
- [30] William Feller. *An introduction to probability theory and its applications*, volume II. Wiley, New York;Sydney;, 1950.
- [31] Elliott W Montroll and John T Bendler. On levy (or stable) distributions and the williams-watts model of dielectric relaxation. *Journal of Statistical Physics*, 34(1):129–162, 1984.
- [32] V. M. Zolotarev. *One-dimensional stable distributions*, volume 65. American Mathematical Society, Providence, R.I, 1986. ISBN 9780821845196;0821845195;.
- [33] Rosario Nunzio Mantegna. Fast, accurate algorithm for numerical simulation of levy stable stochastic processes. *Physical Review E*, 49(5):4677, 1994.
- [34] John Nolan. *Stable distributions: models for heavy-tailed data*. Birkhauser New York, 2003.
- [35] William Feller. *An introduction to probability theory and its applications*, volume 2. Wiley, New York;Sydney;, 1950.
- [36] Neil F. Johnson, Paul Jefferies, and Pak M. Hui. *Financial market complexity*. Oxford University Press, Oxford, 2003. ISBN 0191712108;9780191712104;.
- [37] John P Nolan. Maximum likelihood estimation and diagnostics for stable distributions. *Levy Processes: Theory and Applications*, pages 379–400, 2001.
- [38] John P Nolan. Multivariate elliptically contoured stable distributions: theory and estimation. *Computational Statistics*, 28(5):2067–2089, 2013.
- [39] Yingjie Liang and Wen Chen. A survey on computing levy stable distributions and a new matlab toolbox. *Signal Processing*, 93(1):242–251, 2013.
- [40] John P Nolan. Modeling financial data with stable distributions. *Handbook of Heavy Tailed Distributions in Finance, Handbooks in Finance: Book*, 1:105–130, 2003.
- [41] Rosario N Mantegna and H Eugene Stanley. Stochastic process with ultraslow convergence to a gaussian: the truncated levy flight. *Physical Review Letters*, 73(22):2946, 1994.
- [42] Ismo Koponen. Analytic approach to the problem of convergence of truncated levy flights towards the gaussian stochastic process. *Physical Review E*, 52(1):1197, 1995.
- [43] Giovanni L Vasconcelos. A guided walk down wall street: an introduction to econophysics. *Brazilian Journal of Physics*, 34(3B):1039–1065, 2004.
- [44] Boris Podobnik, Kaushik Matia, Alessandro Chessa, Plamen Ch Ivanov, Youngki Lee, and H Eugene Stanley. Time evolution of stochastic processes with correlations in the variance: stability in power-law tails of distributions. *Physica A: Statistical Mechanics and its Applications*, 300(1-2):300–309, 2001.
- [45] Bwo-Nung Huang. Do asian stock market prices follow random walks? evidence from the variance ratio test. *Applied Financial Economics*, 5(4):251–256, 1995.
- [46] Cheng F Lee, Gong-meng Chen, and Oliver M Rui. Stock returns and volatility on china’s stock markets. *Journal of Financial Research*, 24(4):523–543, 2001.
- [47] Boris V. Gnedenko and A. N. Kolmogorov. *Limit distributions for sums of independent random variables*. Addison-Wesley Pub. Co, Cambridge, Mass, 1954.
- [48] Leo Breiman. *Probability*. Addison-Wesley Pub. Co, Reading, Mass, 1968.
- [49] Benoit Mandelbrot. The variation of certain speculative prices. *The Journal of Business*, 36(4):394–419, 1963.
- [50] Vladimir V. Uchaikin and Vladimir M. Zolotarev. *Chance and Stability: Stable Distributions and their Applications*. De Gruyter, Berlin ;Boston, 2011. ISBN 311093597X;9783110935974;.
- [51] David Applebaum. *Lévy processes and stochastic calculus*. Cambridge university press, 2009.
- [52] Jean Bertoin. *Lévy processes*, volume 121. Cambridge University Press, Cambridge;New York;, 1996. ISBN 0521646324;0521562430;9780521562430;9780521646321;.
- [53] SM Samuels. Infinitely divisible distributions. 1975.
- [54] Achim Klenke. Infinitely divisible distributions. In *Probability Theory*, pages 331–349. Springer, 2014.
- [55] Gennady Samorodnitsky and Murad S. Taqqu. *Stable non-Gaussian random processes: stochastic models with infinite variance*. 1994. ISBN 0412051710;9780412051715;.
- [56] Barry C. Arnold and Dean L. Isaacson. On normal characterizations by the distribution of linear forms, assuming finite variance. *Stochastic Processes and their Applications*, 7(2):227 – 230, 1978. ISSN 0304-4149. doi: [http://dx.doi.org/10.1016/0304-4149\(78\)90019-4](http://dx.doi.org/10.1016/0304-4149(78)90019-4).
- [57] Eric W. Weisstein. *CRC concise encyclopedia of mathematics*. CRC Press, Boca Raton, Fla, 1999. ISBN 9780849396403;0849396409;.
- [58] Michael Feldman. Hilbert transform in vibration analysis. *Mechanical Systems and Signal Processing*, 25(3):735–802, 2011.
- [59] Walter Gander and Walter Gautschi. Adaptive quadrature—revisited. *BIT Numerical Mathematics*, 40(1):84–101, 2000.
- [60] Kaoru Yoneda. Riemann—lebesgue theorem. *Analysis Mathematica*, 7(4):297–302, 1981.
- [61] Robert G Bartle. Return to the riemann integral. *The American Mathematical Monthly*, 103(8):625–632, 1996.
- [62] Milton Abramowitz and Irene A. Stegun. *Handbook of mathematical functions with formulas, graphs, and mathematical tables*. Dover Publications, New York, 1965.
- [63] Armido R DiDonato and Alfred H Morris Jr. Computation of the incomplete gamma function ratios and their inverse. *ACM Transactions on Mathematical Software (TOMS)*, 12(4):377–393, 1986.
- [64] Richard Barakat. Evaluation of the incomplete gamma function of imaginary argument by chebyshev polynomials. *Mathematics of Computation*, pages 7–11, 1961.
- [65] John William Pearson. *Computation of hypergeometric functions*. PhD thesis, University of Oxford, 2009.
- [66] Carl M. Bender and Steven A. Orszag. *Advanced mathematical methods for scientists and engineers*. Springer,

- New York, 1999. ISBN 9780387989310;0387989315;.
- [67] Hans-Gorg Roos, Martin Stynes, and Lutz Tobiska. *Robust numerical methods for singularly perturbed differential equations: convection-diffusion-reaction and flow problems*, volume 24. Springer Science & Business Media, 2008.
- [68] Mark H Holmes. *Introduction to perturbation methods*, volume 20. Springer Science Business Media, 2012.